Available online at www.sciencedirect.com
ScienceDirect
Thin Solid Films 515 (2007) 5374–5380
www.elsevier.com/locate/tsf

Formation and characterization of thin films from phthalocyanine complexes: An electrosynthesis study using the atomic-force microscope

M.E. Sánchez Vergara [a,*], I.F. Islas Bernal [b], M. Rivera [b], A. Ortíz Rebollo [c], J.R. Alvarez Bada [d]

[a] *Departamento de Ingeniería Mecatrónica, Escuela de Ingeniería, Universidad Anáhuac del Norte, Avenida Lomas de la Anáhuac s/n, Col. Lomas Anáhuac, 52786, Huixquilucan, Mexico*
[b] *Instituto de Física, Universidad Nacional Autónoma de México, Circuito Exterior, Ciudad Universitaria, 04510, México D.F., Mexico*
[c] *Instituto de Investigaciones en Materiales, Universidad Nacional Autónoma de México, A.P. 70-360, Coyoacán, 04510, México, D.F., Mexico*
[d] *Instituto Tecnológico y de Estudios Superiores de Monterrey, Campus Ciudad de México, Calle del Puente 222, Col. Ejidos de Huipulco, 14380, México D.F., Mexico*

Received 30 August 2006; received in revised form 13 December 2006; accepted 17 January 2007
Available online 24 January 2007

Abstract

(μ-Cyano)(phthalocyaninato)metal(III) $[PcMCN]_n$ species with a central transition metal ion, such as Fe(III) and Co(III), were used to prepare molecular films on a highly oriented pyrolytic graphite electrode substrate by using the cyclic voltammetry technique. In order to investigate the influence of the ligand on the film properties, 1,8-dihydroxyanthraquinone and 2,6-dihydroxyanthraquinone as bivalent ligands were employed. The structure of the molecular materials was analyzed by infrared spectroscopy. The *in situ* film formation, texture, composition and conductivity of each film were further investigated using atomic force microscopy, scanning electron microscopy, energy-dispersive X-ray spectroscopy and the four-probe technique, respectively. The $[PcMCN]_n$ complexes provided conductive films with an electrical conductivity of $1\times10^{-6}\,\Omega^{-1}\,cm^{-1}$ at 298 K.
© 2007 Elsevier B.V. All rights reserved.

Keywords: Phthalocyanines; Atomic force microscopy; Electrical properties; Conductivity; Optical properties

1. Introduction

Since the discovery of highly-electrically-conducting charge transfer complexes [1,2] and anion-radical salts of tetracyanoquinodimethane (TCNQ) [3,4], several attempts have been performed to design conductor molecular materials. Nowadays, it is well known that several criteria such as the size, shape and intrinsic properties of the component molecules, among others, are critical to achieve the metallic conductivity characteristics of these molecular compounds. Recently, species such as phthalocyanine complexes have been extensively used to construct materials with conductive characteristics, given their wide range of coordination, optical, structural and electronic properties arising from their large π-conjugated systems and their assembling into cofacially-stacked arrays [5–8]. In particular, metallic phthalocyanines have been employed to produce low-dimensional conductive materials upon oxidation [8]. Moreover, molecular conductors have been created by modifying the ligand and the metal ion present in the core of the molecules [9,10]. For instance, the introduction of axial coordinated ligands to the central metal atom has a strong influence on the π-electron conjugation of the macromolecule. Furthermore, the axial substitution exhibits several effects, such as modifying the electronic structure of the phthalocyanine and varying the spatial relationship between neighboring molecules via steric effects and thus, the magnitude of the intermolecular interactions, among others. It has also been observed that large axial coordinated ligands are able to change the packing of the molecules in the solid state and their tendency to aggregate in solution. In addition, it has been noticed that, upon combination of the core metallic ion in a molecular chain, special properties such as the electrical conductivity of a compound can be modified [10,11].

Recent research work has been oriented to the formation and characterization of molecular material thin films [12]. The use of

* Corresponding author. Tel./fax: +52 55 56270210x8236.
E-mail address: elena.sanchez@anahuac.mx (M.E. Sánchez Vergara).

0040-6090/$ - see front matter © 2007 Elsevier B.V. All rights reserved.
doi:10.1016/j.tsf.2007.01.033

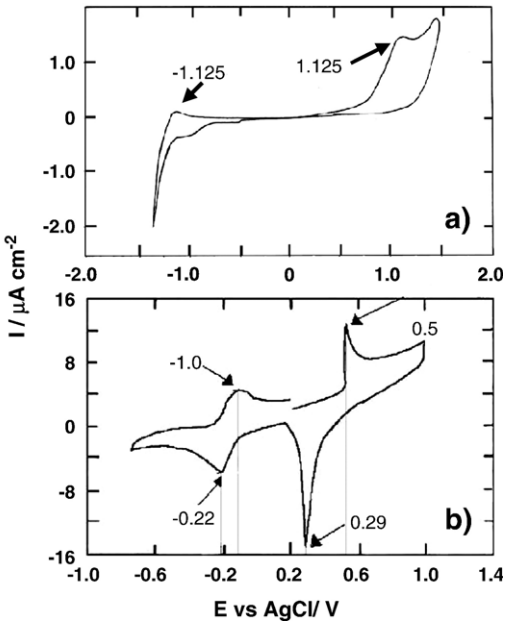

Fig. 1. Cyclic voltammetry of the (a) 1,8-dihydroxyanthraquinone and (b) $[PcFeCN]_n$ species. Potential scan rate 75 mV s^{-1}.

chemical vapor deposition to grow thin films of molecular conductors such as tetrathiafulvalene-tetracyanoqunodimethane (TTF-TCNQ) has been reported [12–14]. On the other hand, phthalocyanines dissolved in organic solvents have been employed to produce thin films through redox processes, showing excellent electrical properties, including the ability to form resilient, semi-conducting thin films and the capability to undergo molecular and structural modifications, it may be desirable to control some of these properties [15,16]. It should also be remarked that the phthalocyanines dissolved in organic solvents have been reduced or oxidized to produce thin films [16].

Thus, in order to investigate the electrochemical reaction and the film formation of cyano(phthalocyaninato)metal(III) $[PcMCN]_n$ species with a central transition metal ion with an open d-shell configuration, such as Co(III) or Fe(III), the organic compounds 1,8 dihydroxyanthraquinone and 2,6 dihydroxyanthraquinone as bivalent ligands were employed. Cyclic voltammetry, combined with atomic force microscopy (AFM), was used for the film formation and surface characterization, among others.

2. Experimental details

The compounds 1,8-dihydroxyanthraquinone and 2,6-dihydroxyanthraquinone were used from commercial suppliers and used without further purification. The complexes (μ-cyano)

Table 1
IR data for all the compounds as thin films

Compound	IR (CN^-)	IR (C═O)	IR (C–O)
1	–	1606 cm^{-1}	1089 cm^{-1}
2	–	1598 cm^{-1}	1332 cm^{-1}
3	–	1609 cm^{-1}	1085 cm^{-1}
4	–	1615 cm^{-1}	1322 cm^{-1}

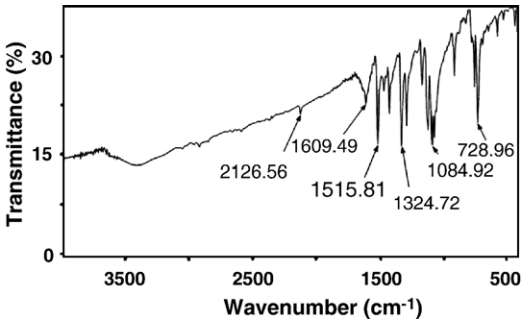

Fig. 2. IR spectrum obtained for compound (3).

(phthalocyaninate)M(III) or $[PcMCN]_n$ where M=Fe, Co were synthesized from iron(III) phthalocyanine chloride and cobalt(II) phthalocyanine as reported elsewhere [17].

The initial stages of electrochemical deposition by using cyclic voltammetry and the AFM surface characterization were carried out *in situ* in the electrochemical (EC) fluid cell of an atomic force microscope, Nanoscope IIIa Digital Instrument. Here, highly oriented pyrolytic graphite (HOPG) was used as a working electrode, platinum wire as a counter electrode and silver wire as a reference electrode. The EC-AFM experiments were run using cyclic voltammetry between the cathodic (−1.0 V) and anodic (+1.0 V) switching potentials. The potential scan rate was 75 mV s^{-1} in all cases. The morphological

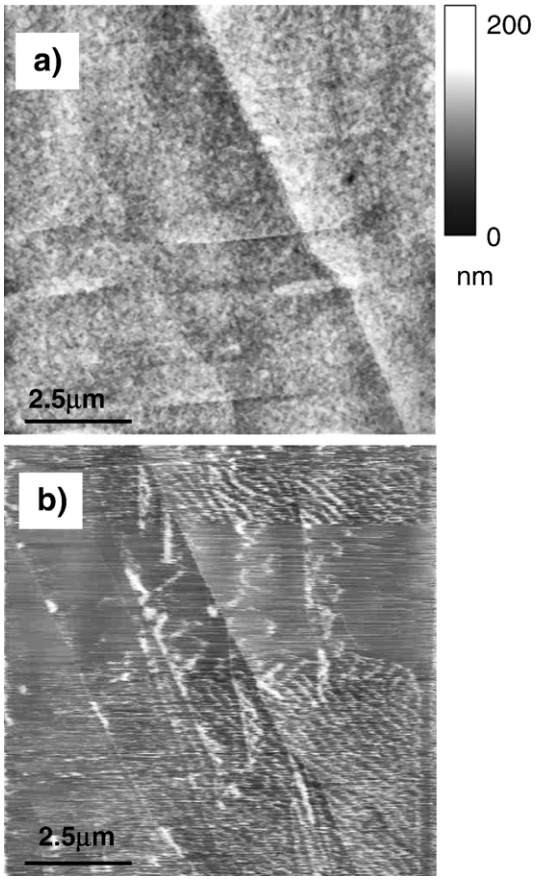

Fig. 3. In situ AFM images of the electrode surface after (a) 0 and (b) 20 PSC for the $[PcFeCN]_n$ and 1,8-dihydroxyanthraquinone complex. Image sizes are 10×10 μm.

characterization by AFM of the electrodeposited materials was performed *in situ* in the contact mode using low scanning forces (0.3 N m^{-2}) at the open circuit mode. For this study, 0.1 M tetrabutylammonium tetrafluoroborate was used as support electrolyte and the phthalocyanines were dissolved in absolute ethanol with a 0.01 M concentration [17]. The AFM characterization of the electrodeposited material was performed in the presence of the aqueous electrolyte (50 μl). In order to compare the electrode surface modification before and after deposition, the HOPG was imaged before the electrochemical reactions and after different potential scan cycles (PSC).

Elemental analysis of the electrodeposited films was performed with a Jeol JSM5900 scanning electron microscope (SEM) coupled to an energy-dispersive spectrophotometer (EDS) working at 20 keV. The acquisition of the EDS data was stopped when it reached 5000 counts. The infrared spectra were obtained by using a Perkin Elmer 282-B IR spectrophotometer. The spectra were recorded by the KBr-pellet technique. Finally, the electric conductivity of the films was studied by means of a four-point probe; for these measurements, the molecular films onto the HOPG substrates were analyzed by using four metallic strips that acted as electrodes. In order to get an ohmic behaviour between the deposited films and the metallic electrodes, four gold or silver strips were deposited by vacuum thermal evaporation onto the glass slices. To prevent the strips from reaching the surface of the substrate, a molybdenum boat with two grids was used as the evaporation source. The boat temperature was 473 °C during evaporation, as measured with a chromel–alumel thermocouple. The electric current as a function of temperature was measured with an applied voltage of 100 V in the ohmic regime by using a Keithley 230 programmable voltage source and a Keithley 485 peak-ammeter coupled to an HP3421 data collector.

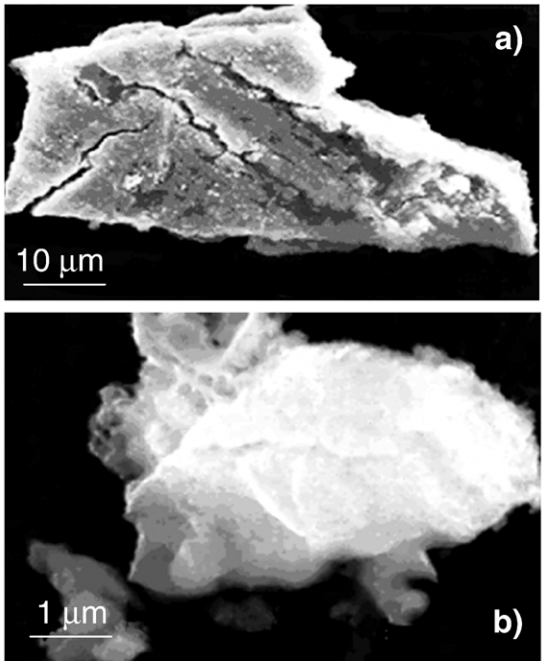

Fig. 4. SEM image of the $[PcFeCN]_n$ (a) 1,8-dihydroxyanthraquinone and (b) 2,6-dihydroxyanthraquinone complex electrodeposited on the HOPG surface after 60 PSC.

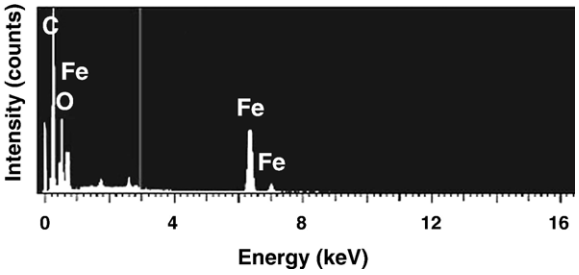

Fig. 5. EDS analysis of the $[PcFeCN]_n$ and 1,8-dihydroxyanthraquinone material electrodeposited onto HOPG after 60 PSC.

3. Results and discussion

Cyclic voltammetry was performed on the starting compounds to investigate their redox properties individually. From this information, it was possible to investigate their ability to electrodeposit material by themselves as well as to infer a possible molecular material formation from the mixtures. The cyclic voltammetry response of the 1,8-dihydroxyanthraquinone and the $[PcFeCN]_n$ system is shown in Fig. 1a, b, respectively.

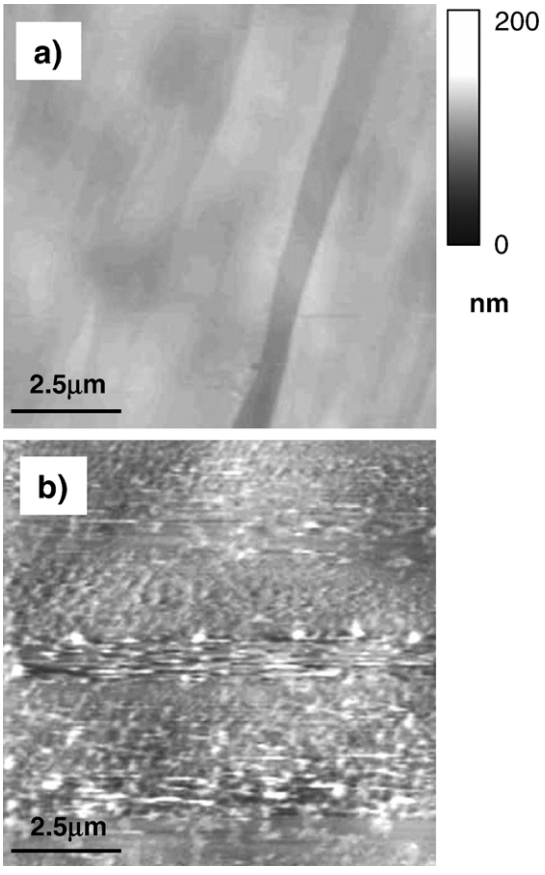

Fig. 6. In situ AFM images of the $[PcFeCN]_n$ and 2,6-dihydroxyanthraquinone film on the electrode surface after (a) 0 and (b) 20 PSC. Image sizes are 10×10 μm.

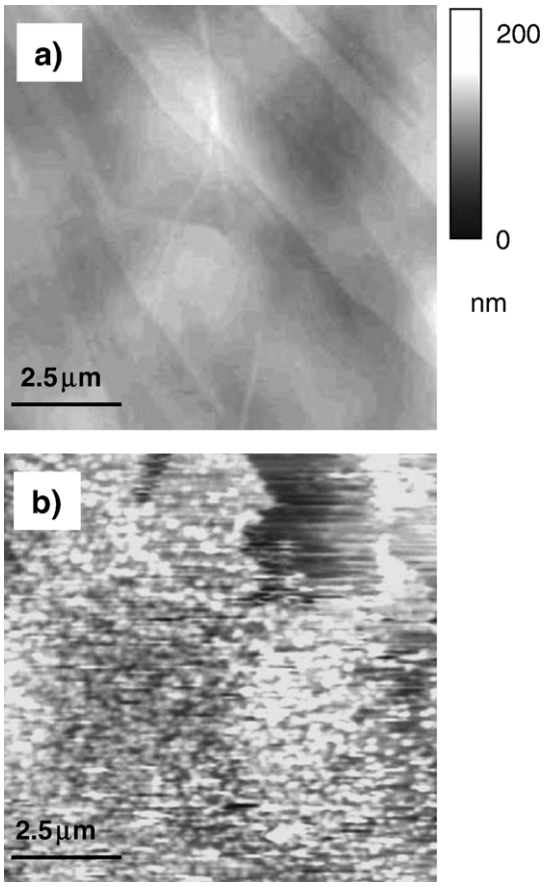

Fig. 7. In situ AFM images of the $[PcCoCN]_n$ and 1,8-dihydroxyanthraquinone film after (a) 0 and (b) 20 PSC. Image sizes are 10×10 μm.

From the cyclic voltammetry plot, anodic and cathodic peak currents are observed in both cases. From the redox peak values of both compounds, it was possible to find the appropriate potential difference for the formation of molecular materials in the electrosynthesis cells and the EC-AFM fluid cell as suggested by the Saito and Ferraris criterion [18]. This analysis was performed on each of the starting compounds and similar results were found. It is important to mention that the starting solutions were in contact with the HOPG surface for some minutes before the redox process began in order to investigate their spontaneous adsorption on the electrode. In all cases, a very light adsorption took place after 20 min, as seen by AFM, but it was negligible in comparison with the electrodeposited material formed from the redox mechanism.

In order to obtain molecular materials from the reaction mechanism of the starting compounds, it was necessary to modify the coordination state of the metal in the phthalocyanines. For instance, a cyano group was added to the fifth and sixth positions of the coordination sphere of the metallic central ion $[PcMCN]_n$ where M=Fe, Co [17]. Furthermore, the anisotropic character and the formation of long symmetric chains to obtain molecular materials were probed by replacing the cyano groups of the metallic ion with the organic species. IR spectroscopy results of the materials formed by electrocrystallization within the organic–inorganic reaction mechanism are shown in Table 1. From these results, one can notice that the material from the $[PcCoCN]_n$ and 1,8-dihydroxyanthraquinone species (1) exhibits C═O and C–O functional groups with wavelengths of 1606 cm^{-1} and 1089 cm^{-1}, respectively. On the other hand, the absence of the 2158 cm^{-1} wavelength corresponding to the cyano group of the $[PcCoCN]_n$, supports the idea that the cyano group has been substituted by the 1,8-dihydroxyanthraquinone species in the fifth and sixth positions of the coordination sphere of the cobalt. For the $[PcCoCN]_n$ and 2,6-dihydroxyanthraquinone reaction, the material (2) exhibited two signals associated to the C═O and C–O groups with wavelengths of 1598 cm^{-1} and 1332 cm^{-1}, respectively. Again, the absence of the 2158 cm^{-1} wavelength supports the substitution of the cyano group with the organic species. Similar results were obtained for the $[PcFeCN]_n$ compound with the 1,8-dihydroxyanthraquinone (3) and the 2,6-dihydroxyanthraquinone (4) species, respectively. Fig. 2 shows the IR spectrum obtained for compound (3).

AFM images of the HOPG electrode surface after the $[PcFeCN]_n$ and 1,8-dihydroxyanthraquinone (3) reaction showed a modification of the interface due to the presence of material as we can see in Fig. 3. The sequence shows, for the HOPG, (a) the initial surface and (b) after 20 PSC, respectively. From these images, the presence of scattered features is clear. The RMS roughness analysis of the interface showed roughness values of 1.90 nm and 3.31 nm, respectively. From these numbers, it is clear that a modification of the electrode took place in spite of the material thickness being very thin, which suggests the formation of tiny amounts of the electrodeposited

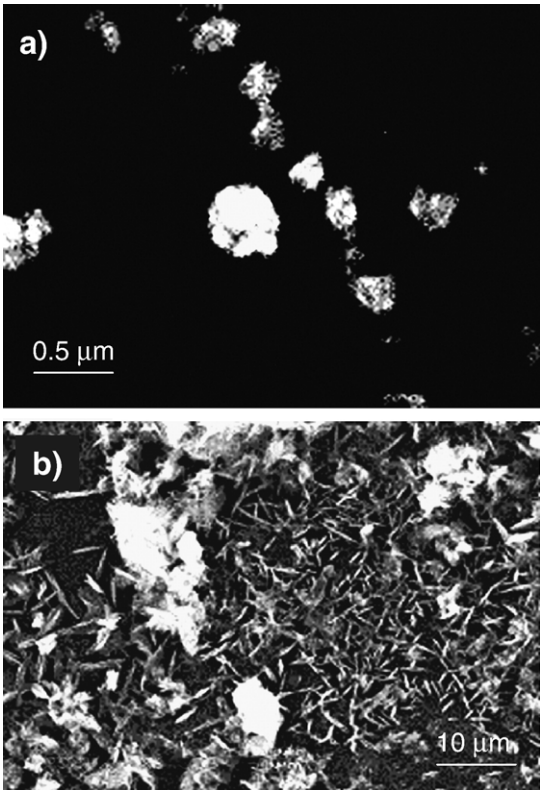

Fig. 8. SEM image of the $[PcCoCN]_n$ (a) 1,8-dihydroxyanthraquinone and (b) 2,6-dihydroxyanthraquinone complex electrodeposited on the HOPG surface after 60 PSC.

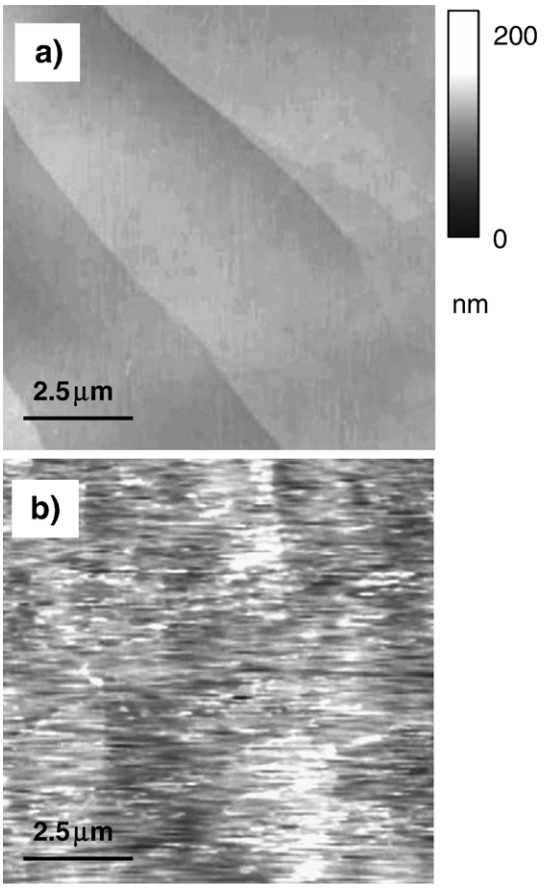

Fig. 9. In situ AFM images of the $[PcCoCN]_n$ with 2,6-dihydroxyanthraquinone complex after (a) 0 and (b) 20 PSC. Image sizes are 10×10 μm.

compound. SEM (Fig. 4a) and EDS (Fig. 5) analyses were performed *ex situ* after several potential scan cycles. These results showed a homogeneous but irregular electrodeposit material where the presence of the starting elements can be noticed. For instance, the presence of iron from the $[PcFeCN]_n$ molecule and oxygen from the 1,8-dihydroxyanthraquinone species were observed. It is worth to mention that the largest

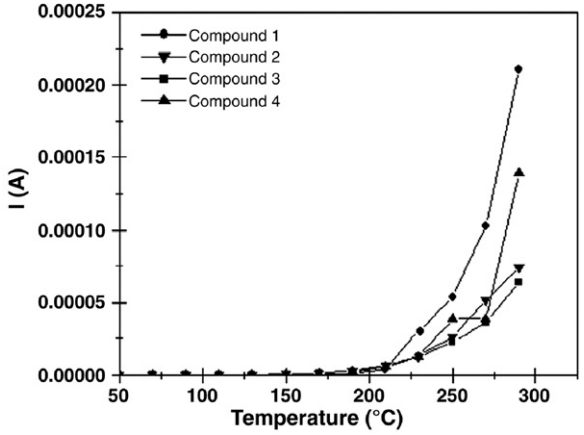

Fig. 10. Electric current vs. temperature for the thin films from the cobalt (1, 2) and iron (3, 4) compounds.

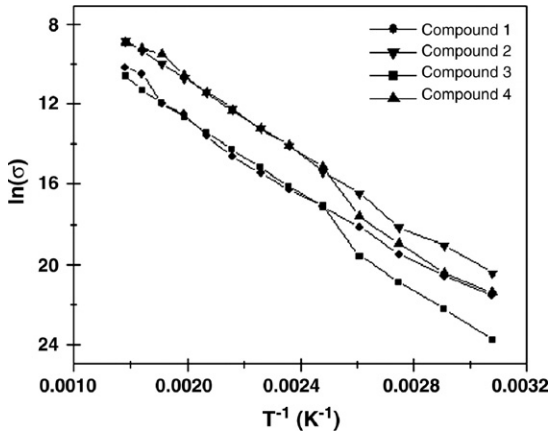

Fig. 11. Electrical conductivity as a function of inverse temperature for the thin films from the cobalt (1, 2) and iron (3, 4) compounds.

amount of carbon found in the sample came from the electrode surface (HOPG), as it is entirely composed of carbon atoms.

When we combined the $[PcFeCN]_n$ with the 2,6-dihydroxyanthraquinone salt (4), we observed some material electrodeposited on the HOPG surface. From Fig. 6, the HOPG surface (a) before and (b) after 20 PSC of electrodeposition is shown. Roughness analysis of the electrode interface showed a minimal roughness change from 5.2 nm to 5.3 nm. A closer view of the surface shows the presence of tiny spots irregularly distributed on the electrode area; SEM analysis confirms this morphology (Fig. 4b). After several PSC, EDS analyses were similar to the $[PcFeCN]_n$ compound with the 1,8-dihydroxyanthraquinone since the presence of iron from the $[PcFeCN]_n$ molecule and oxygen from the anthraquinone species was observed.

On the other hand, the $[PcCoCN]_n$ with the 1,8-dihydroxyanthraquinone species (1) produced a thin rough film. The AFM images are shown in Fig. 7. Here, (a) the bare substrate and (b) the surface after 20 PSC are displayed. The surface modification is clear from these images since it is partially covered with the obtained material with roughness values from 4.3 nm to 9.3 nm, respectively. Although the surface modification as seen with AFM after few PSC showed a very smooth coverage, SEM and EDS images showed the presence of small aggregates on the electrode after several PSC (Fig. 8a) with a composition including the elements of the starting compounds: cobalt from the $[PcCoCN]_n$ molecule and oxygen from the anthraquinone.

Finally, the complex formed from $[PcCoCN]_n$ with the 2,6-dihydroxyanthraquinone salt (2) is shown in Fig. 9. AFM images of (a) the initial surface and (b) after 20 PSC of

Table 2
Electric current, resistance and electrical conductivity of synthesized materials at 25 °C with 100 V ohmic voltage

Compound	Electrical current I (A)	Resistance R (Ω)	Electrical conductivity σ (Ω^{-1} cm^{-1})
1	1.13×10^{-10}	8.85×10^{11}	3.48×10^{-6}
2	4.58×10^{-10}	2.18×10^{11}	1.12×10^{-5}
3	5.51×10^{-11}	1.82×10^{12}	2.50×10^{-6}
4	6.41×10^{-10}	1.56×10^{11}	1.69×10^{-5}

Table 3
Optical and electrical activation energies for the molecular materials' thin films

Compound	ΔE_m (eV)
1	1.50
2	3.60
3	1.55
4	2.15

electrodeposition display a smooth surface modification. The roughness numbers for these surfaces changed from 3.3 nm to 4.2 nm. On the other hand, *ex situ* SEM images and EDS analysis showed the formation of small aggregates and needles (polycrystalline aggregates) on the electrode surface (Fig. 8b) where the presence of reference elements was observed after several PSC.

The variation of electrical current with temperature on thin films was evaluated by using the four-probe method, in order to investigate the electrical behavior of the synthesized materials. This is one of the most used techniques for resistivity measurements at the semiconductor industry. The measurement took place in a line on the material having equal spaces between the test points. Care must be taken that the current involved be low enough to prevent sample heating and the voltmeter must have high input impedance.

Fig. 10 shows the electric current variation through the films as the temperature increases, at a constant applied voltage in the ohmic regime for thin films of each synthesized molecular material. The plots for all four molecular materials indicate a semiconductor behavior, being the (1) compound the more conductive above 280 °C while, at low temperatures, its behavior is like that of the other materials.

Fig. 11 shows the semiconductor behavior of the synthesized materials. It can be observed that the conductivity increases with temperature in all cases. The electrical conductivity and resistivity results were evaluated for all compounds at 25 °C. The results are shown in Table 2, where compound (1) shows the highest conductivity value. The electrical conductivity values at room temperature for all materials are within the ranges commonly observed in semiconductor materials (10^{-6} to 10^{1} Ω^{-1} cm^{-1}) [19]. This is important since a molecular semiconductor is generally defined in terms of its conductivity at room temperature and its temperature-dependent behavior, which can be related to impurity types, location and concentration, structure, stacking and orbital overlap.

This behavior indicates that the electrical conductivity $\sigma(T)$ is thermally activated and is assumed to arise from the contribution due to conduction between extended states. This behavior is described by the Arrhenius law in the form:

$$\sigma = \sigma_m \exp\left(-\frac{\Delta E_m}{KT}\right)$$

Where σ_m is the pre-exponential factor and ΔE_m is the activation energy for electrical conductivity. Calculated values of ΔE_m are shown in Table 3. The quantity ΔE_m is an activation energy involving both the energy necessary to excite electrons from the localized states towards extended states through the mobility edge and the electrical conduction by means of the hopping mechanism between localized states. Taking into account the optical and electrical properties of the deposited films, it may be possible to consider this material for electronic-device applications.

4. Conclusions

The formation of molecular materials from Fe(III) and Co(III) phthalocyanines was achieved using electrosynthesis methods. Although both compounds electrodeposited materials when they were combined with the 1,8-dihydroxyanthraquinone and the 2,6-dihydroxyanthraquinone salts, only small differences were observed. For instance, the 1,8-dihydroxyanthraquinone electrodeposited slightly more material than the 2,6-dihydroxyanthraquinone salt, though both of them produced initially very thin films.

AFM results provide an important evidence of electrodeposition in the early stages of growth since the thin film thickness obtained with this method is difficult to observe using any other technique. On the other hand, AFM images exhibited valuable information about the film growth process when small amounts of material and shorter times were employed. This is important to understand the electronic properties of the films in terms of the homogeneity and surface coverage of the working electrode. AFM, as well as other complementary techniques such as SEM and EDS, provided evidence of the formation of molecular materials in a micro-scale that can be extrapolated to typical electrosynthesis cells in order to obtain larger amounts of these materials.

The films obtained were found to be semiconductors with conductivities in the 10^{-6}–10^{-5} Ω^{-1} cm^{-1} range at room temperature. The value of the calculated activation energies, the order of magnitude of the electrical conductivities and the possibility to prepare thin films from these materials suggest that it may be possible to use them in the preparation of electronic devices.

Acknowledgments

The authors acknowledge Dr. José D. Sepulveda-Sánchez at UAM-Iztapalapa for SEM and EDS technical assistance and Dr. Abel Moreno at IQ–UNAM, México, for providing the AFM facilities. M.E. Sánchez Vergara and I.F. Islas Bernal acknowledge financial support from CONACYT, México (grant number 36715-U). M. Rivera acknowledges financial support from UNAM, México (PAPIIT grant number IN-112106).

References

[1] J. Ferraris, D.O. Cowan, V.J. Walatka, J.H. Perlstein, J. Am. Chem. Soc. 95 (1973) 948.
[2] L.B. Coleman, M.J. Cohen, D.J. Sandman, F.G. Yamagishi, A.F. Garito, A.J. Heeger, Solid State Commun. 12 (1973) 1225.
[3] L.R. Melby, R.J. Harder, W.R. Hertler, W. Mahler, R.E. Benson, W.E. Mochel, J. Am. Chem. Soc. 84 (1962) 3374.
[4] L.I. Buravov, D.N. Fedutin, I.F. Shchegolev, Sov. Phys. JETP 32 (1971) 612.

[5] C.C. Leznoff, A.B.P. Lever, Phthalocyanines: Properties and Applications, VCH Publishers, USA, 1989.
[6] N.B. McKeown, Phthalocyanine Materials: Structure, Synthesis and Function, Cambridge University Press, UK, 1998.
[7] T. Inabe, Y. Maruyama, Bull. Chem. Soc. Jpn. 63 (1990) 2273.
[8] T. Inabe, T.J. Marks, R.L. Burton, J.W. Lyding, W.J. McCarthy, C.R. Kannewurf, G.M. Reisner, R.H. Herbestein, Solid State Commun. 54 (1985) 501.
[9] O. Bekaroglu, Appl. Organomet. Chem. 10 (1996) 605.
[10] N.B. McKeown, J. Mater. Chem. 10 (2000) 1979.
[11] M. Hanack, Inorg. Organomet. Polym. II 572 (1994) 472.
[12] P. Cassoux, D. De Caro, L. Valade, H. Casellas, B. Daffos, M.E. Sánchez Vergara, Mol. Cryst. Liq. Cryst. Sci. Technol., Sect. A Mol. Cryst. Liq. Cryst. 380 (2002) 45.
[13] J. Caro, S. Garelik, A. Figeras, Chem. Vap. Depos. 2 (1996) 251.
[14] A. Figueras, J. Cryst. Growth 166 (1996) 798.
[15] S. Kim, J. Porphyr. Phthalocyanines (2000) 136.
[16] P.L. Boulas, M. Gomez-Kaifer, L. Echegoyen, Angew. Chem., Int. Ed. Engl. 37 (1998) 216.
[17] J. Metz, M. Hanack, J. Am. Chem. Soc. 105 (1983) 828.
[18] G. Saito, J. Ferraris, Bull. Chem. Soc. Jpn. 53 (1980) 2141.
[19] J. Simon, F. Tournillac, New J. Chem. 11 (1997) 383.